Cas9-mediated endogenous plasmid loss in *Borrelia burgdorferi*

Constantin N. Takacs[1,2,3], Yuko Nakajima[4], James E. Haber[4], and Christine Jacobs-Wagner[1,2,3,*]

[1]Department of Biology, Stanford University, Palo Alto, CA 94305.

[2]Sarafan ChEM-H Institute, Stanford University, Palo Alto, CA 94305.

[3]Howard Hughes Medical Institute, Stanford University, Palo Alto, CA 94305.

[4]Department of Biology and Rosenstiel Basic Medical Sciences Research Center, Brandeis University, Waltham, MA 02454.

*Corresponding author: jacobs-wagner@stanford.edu.

ABSTRACT

The spirochete *Borrelia burgdorferi,* which causes Lyme disease, has the most segmented genome among known bacteria. In addition to a linear chromosome, the *B. burgdorferi* genome contains over 20 linear and circular endogenous plasmids. While many of these plasmids are dispensable under in vitro culture conditions, they are maintained during the natural life cycle of the pathogen. Plasmid-encoded functions are required for colonization of the tick vector, transmission to the vertebrate host, and evasion of host immune defenses. Different *Borrelia* strains can vary substantially in the type of plasmids they carry. The gene composition within the same type of plasmid can also differ from strain to strain, impeding the inference of plasmid function from one strain to another. To facilitate the investigation of the role of specific *B. burgdorferi* plasmids, we developed a Cas9-based approach that targets a plasmid for removal. As a proof-of-principle, we showed that targeting wild-type Cas9 to several loci on the endogenous plasmids lp25 or lp28-1 of the *B. burgdorferi* type strain B31 results in sgRNA-specific plasmid loss even when homologous sequences (i.e., potential sequence donors for DNA recombination) are present nearby. Cas9 nickase versions, Cas9^{D10A} or Cas9^{H840A}, also cause plasmid loss, though not as robustly. Thus, sgRNA-directed Cas9 DNA cleavage provides a highly efficient way to eliminate *B. burgdorferi* endogenous plasmids that are non-essential in axenic culture.

INTRODUCTION

Lyme disease, also known as Lyme borreliosis, is the most prevalent vector-borne disease in North America and Eurasia [1, 2]. It is caused primarily by the spirochete *Borrelia burgdorferi* and the related *Borrelia afzelii* and *Borrelia garinii* species. The disease presents with various symptoms that can include fever, malaise, rash, arthritis, neurological dysfunctions, and cardiac manifestations [3]. Humans are accidental hosts. In nature, *B. burgdorferi* is typically maintained through a transmission cycle

between a vertebrate host reservoir (e.g., white footed mice and other small mammals, but also birds) and an ixodid tick vector [4]. During feeding, *B. burgdorferi*-colonized tick vectors deliver the spirochetes into vertebrate hosts, where the spirochetes can replicate, disseminate, and often establish persistent infection.

Members of the Borreliaceae family contain the most segmented bacterial genomes known to date [5]. For instance, the genome of the *B. burgdorferi* type strain B31 is composed of a linear chromosome and 21 linear and circular plasmids [6, 7]. During growth, the Borreliaceae are polyploid, as each cell carries multiple copies of both the chromosome and plasmids [8, 9]. The chromosome encodes the vast majority of essential housekeeping and metabolic functions [6, 10]. In contrast, the plasmids primarily encode lipoproteins that mediate the spirochetes' interaction with the vertebrate and tick host environments and help them evade host immune defenses [6, 7, 11-16]. Additionally, each strain hosts several highly similar plasmid members of the cp32 class, which are prophages [7, 17-20]. In the *B. burgdorferi* type strain B31, which is the most well studied genetically, only plasmid cp26 has been shown to be required for growth in axenic culture [21-24]. Several other plasmids are known to be required in the vertebrate or tick hosts [4, 25, 26]. However, much remains unknown about the roles of *B. burgdorferi* plasmids. Furthermore, as the number of distinct plasmid types and the genes carried by any given plasmid type vary significantly among Borreliaceae species and strains [10, 17, 27, 28], strain-to-strain inferences of plasmid function are not always possible.

An effective way to investigate plasmid function is to remove it from a given strain. Spontaneous plasmid loss during extended passaging in axenic culture has been known since the early days of Lyme disease research [29, 30], but this approach is not specific to a particular plasmid of interest and often

results in loss of multiple plasmids [25, 26, 31, 32]. Curing a specific plasmid can be achieved through transformation of *B. burgdorferi* with a shuttle vector that carries the plasmid maintenance locus of the endogenous plasmid of interest [33]. The incompatibility that arises between the endogenous plasmid and the introduced shuttle vector leads to displacement of the endogenous plasmid by the shuttle vector [33-39]. However, this approach requires knowledge of the plasmid maintenance locus of the targeted endogenous plasmids.

A potentially easier method to eliminate endogenous plasmids from *B. burgdorferi* strains would be to generate site-specific DNA lesions. In the absence of efficient DNA repair, those lesions might lead to degradation of the targeted endogenous plasmid. Indeed, in the absence of a recombinational donor sequence, exogenously induced double-stranded DNA breaks (DSBs) in the chromosome can be lethal in several bacteria, including *Escherichia coli* [40, 41], streptococci [42], *Clostridium cellulolyticum* [43], and the spirochete *Leptospira biflexa* [44]. Repair of a site-specific DSB in *Neisseria gonorrhoeae*, when there are no homologous sequences to provide a template for recombinational repair, occurs at such low frequencies that less than one cell in ten thousands survives this type of genome lesion [45]. In contrast, the presence of short (5 to 23 base pairs) homologous sequences flanking an endonuclease-induced DSB led to RecA-mediated repair in a small fraction of cells [45]. Since most *B. burgdorferi* plasmids are not needed for growth in axenic culture, induction of DNA lesions in *B. burgdorferi* plasmids should cause plasmid loss if DNA repair is inefficient.

To generate such site-specific lesions, we used the clustered regularly interspaced palindromic repeats (CRISPR)-Cas9 system derived from *Streptococcus pyogenes* [46, 47]. Cas9 is the endonuclease component of a type of bacterial innate immunity defense against invading foreign DNA molecules [48].

It has two catalytic residues, D10 and H840, each cutting one of the strands of the targeted double stranded DNA sequence [46]. Cas9 targeting to a specific DNA sequence can be achieved by co-expression of a short guide RNA molecule, or sgRNA. Base pairing between the Cas9-bound sgRNA and the target DNA sequence next to a protospacer-adjacent motif (PAM) directs the Cas9 activity to the genome location specified by the sgRNA [46]. While wild-type Cas9 ($Cas9^{WT}$) generates a DSB in the target DNA sequence, single active site mutants ($Cas9^{D10A}$ and $Cas9^{H840A}$) are nickases that generate single-stranded DNA breaks (SSBs) [46]. Finally, the double mutant, catalytically dead $Cas9^{D10A/H840A}$, or dCas9, does not create DNA lesions and thus serves as a negative control. dCas9, however, can interfere with transcription when targeted to promoters and promoter-proximal coding region [49, 50]. Relying on this transcription-interfering property, a previous report from our laboratory established and characterized a dCas9-based CRISPR interference (CRISPRi) platform in *B. burgdorferi* [51]. Building on that work, we report herein the effects of targeting $Cas9^{WT}$ and its nickase versions to several *B. burgdorferi* endogenous plasmid loci.

RESULTS

Expression and targeting of Cas9 activity in *B. burgdorferi*

The previous report establishing CRISPRi in *B. burgdorferi* relied in part on all-in-one *E. coli* / *B. burgdorferi* shuttle vectors that carry a constitutive sgRNA expression cassette as well as an isopropyl β-D-1-thioglactopyranoside (IPTG)-inducible dCas9 expression cassette [51]. Using these CRISPRi shuttle vectors or control vectors that lack the sgRNA as background, we generated vectors (Fig. 1) that express either $Cas9^{WT}$, which cleaves both DNA strands, or nickases $Cas9^{H840A}$ and $Cas9^{D10A}$, which cleave only one DNA strand [46].

Figure 1. Schematic depiction of *E. coli*/*B. burgdorferi* shuttle vectors used in this study. Left, all-in-one, Cas9-targeting shuttle vectors carrying a sgRNA expression cassette as well as an IPTG-inducible Cas9 expression cassette that contains a constitutively expressed *lacI* gene. Right, non-targeting Cas9 shuttle vectors, which lack the sgRNA cassette. The Cas9 versions used are, from top to bottom: dCas9, $Cas9^{D10A}$, $Cas9^{H840A}$, and $Cas9^{WT}$. The dCas9 shuttle vectors were previously described [51]. Presence of the D10A or H840A mutation is indicated by arrowheads. Features are not drawn to scale. For simplicity, other important features of the shuttle vectors, such as the antibiotic resistance cassette or the *E. coli* or *B. burgdorferi* origins of replication, are not marked on the figure.

In separate cultures, we targeted $Cas9^{WT}$ or its nickase versions to two endogenous *B. burgdorferi* plasmids, lp25 and lp28-1 (Fig. 2). Plasmid lp25 encodes the nicotinamidase PncA which is essential for *B. burgdorferi*'s survival in the tick and vertebrate hosts [25, 34, 52-56]. Plasmid lp28-1 carries the *vls* antigenic variation system, which is composed of the expressed *vlsE* lipoprotein gene and 15 silent *vls* cassettes, *vls2*-*vls16* (Fig. 2A), and is needed for the establishment of persistent infection in immunocompetent vertebrate hosts [11, 57, 58]. For lp28-1, we independently targeted two different sites in *vlsE,* plus one site in one of the silent *vls* cassettes, *vls11*, and another in the non-*vls* locus *bbf03* (Fig. 2A). For lp25, we selected genes *bbe10* and *bbe17* and targeted them individually (Fig. 2B). The sequences of the spacer and the PAM of these sgRNAs are listed in Table 1.

Figure 2. Locations targeted by Cas9 activity in *B. burgdorferi* endogenous plasmids lp28-1 and lp25. A. Top: schematic depiction of plasmid lp28-1. Marked (but not drawn to scale) are gene *bbf03* and the *vls* locus, which were targeted by the indicated sgRNAs. The sgRNAs were used one

at a time, never in combination. Middle: magnification of the *vls* locus. Shown (but not drawn to scale) are the expressed *vlsE* lipoprotein gene and the 15 silent *vls* cassettes. Bottom: magnified view of the *vlsE1* cassette, which contains the variable regions of the expressed *vlsE* lipoprotein, flanked by two direct repeats (DRs). Variable regions (VRs) 1 through 6 are depicted, as well as the locations targeted by sgRNAvlsE1 and sgRNAvlsE2. Covalently closed hairpin telomeres are depicted as ovals flanking both ends of the linear plasmid. **B.** Same as in (A) but for plasmid lp25. Marked (but not drawn to scale) are genes *bbe10* and *bbe17*, which were independently targeted by the indicated sgRNAs. **C.** Depiction of part of the *vlsE* gene of strain K2. Shown in gray are sequences shared with the *vlsE* sequence reported for the parental strain B31. In color are divergent sequences that likely arose by recombination of the indicated silent cassettes into the expressed locus. The colors match those used for the silent cassettes in panel A. The *vls8*/*16* notation signifies a sequence that could have originated from either the *vls8* or *vls16* silent cassette.

Table 1. sgRNAs used in this study

sgRNA ID	Guide RNA spacer sequence (5' to 3')	PAM	*B. burgdorferi* target plasmid
bbe10	AGGGGGAAGACAATTTACTT	TGG	lp25
bbe17	AATATTCTTTCAGGGTAAGC	AGG	lp25
vlsE1	GGATGGAGAGAAGCCTGAGG	AGG	lp28-1
vlsE2	GCTACAGGGGAGAATAATAA	AGG	lp28-1
vls11	GCTGTTAGTGCTGGTTAGTG	TGG	lp28-1
bbf03	AGAGTTTCTACGATTGAGTA	TGG	lp28-1

For these experiments, we used strain B31-A3-68 Δ*bbe02*::P_{flgB}-*aphI*, also known as K2, a transformable, clonal, infectious derivative of the type strain B31 [59]. A mouse passage occurred during the derivation of strain K2 from the parental, sequenced B31 strain [31, 59]. During that mouse passage, gene conversion events likely changed the *vlsE* sequence. We therefore sequenced the entire *vls* locus of strain K2 using long read single-molecule, real-time (SMRT) sequencing [60] to obtain an accurate sequence encompassing the expressed *vlsE* gene and the repetitive silent *vls* cassettes. We

146 found that the sequence of the silent *vls* cassette region was identical to the *B. burgdorferi* B31 reference
147 sequence (GenBank accession number AE000794.2) [6]. In contrast, we found that the sequence of the
148 *vlsE* gene of strain K2 had indeed diverged from the parental B31 *vlsE*, as expected. We detected five
149 clusters of changes that could be attributed to segmental gene conversion events in which the original
150 sequence was replaced by segments copied from the *vls2-vls16* silent cassette sequences (Fig. 2C).
151 Based on the alignment of the K2 *vlsE* sequence with the silent *vls2-16* cassette sequences, we designed
152 two sgRNAs, sgRNAvlsE1 and sgRNAvlsE2, to maximize on-target (*vlsE*) and minimize off-target (the
153 rest of the genome including *vls2-16*) binding potential (Fig. 2C and Table 1). We were unable to
154 generate a shuttle vector carrying both *cas9*^{wt} and sgRNAvlsE2, possibly due to toxicity of DSBs
155 associated with off-target Cas9^{WT} activity in *E. coli*. We did, however, generate shuttle vectors carrying
156 genes encoding dCas9, Cas9^{D10A}, or Cas9^{H840A}, in combination with sgRNAvlsE2. The shuttle vectors
157 containing these constructs are listed in Table 2.
158

159

Table 2. *E. coli/B. burgdorferi* shuttle vectors[a] used in this study

Shuttle vector name	CJW strain number[b]	Selection[c]	Source or Reference
i. Shuttle vectors expressing catalytically inactive dCas9			
pBbdCas9S		Sm/Sp	[51]
pBbdCas9S_arr2		Sm/Sp, Rf	[51]
pBbdCas9S_P_{syn}-sgRNA500		Sm/Sp	[51]
pBbdCas9G_arr2		Gm, Rf	[51]
pBbdCas9S(RBSmut)		Sm/Sp	[51]
pBbdCas9S(RBSmut)_arr2		Sm/Sp, Rf	[51]
pBbdCas9S(RBSmut)_ P_{syn}-sgRNA500		Sm/Sp	[51]
pBbdCas9S(RBSmut)_P_{syn}-sgRNAvlsE1	CJW7267	Sm/Sp	This study
pBbdCas9S(RBSmut)_P_{syn}-sgRNAvlsE2	CJW7268	Sm/Sp	This study
pBbdCas9S(RBSmut)_P_{syn}-sgRNAvls11	CJW7269	Sm/Sp	This study
pBbdCas9S(RBSmut)_P_{syn}-sgRNAbbf03	CJW7282	Sm/Sp	This study
pBbdCas9S(RBSmut)_P_{syn}-sgRNAbbe10	CJW7280	Sm/Sp	This study
pBbdCas9S(RBSmut)_P_{syn}-sgRNAbbe17	CJW7281	Sm/Sp	This study
ii. Shuttle vectors expressing the nickase $Cas9^{D10A}$			
pBbCas9^{D10A}S(RBSmut)	CJW7290	Sm/Sp	This study
pBbCas9^{D10A}S(RBSmut)_arr2	CJW7291	Sm/Sp, Rf	This study
pBbCas9^{D10A}S(RBSmut)_P_{syn}-sgRNA500	CJW7292	Sm/Sp	This study
pBbCas9^{D10A}S(RBSmut)_P_{syn}-sgRNAvlsE1	CJW7293	Sm/Sp	This study
pBbCas9^{D10A}S(RBSmut)_P_{syn}-sgRNAvlsE2	CJW7294	Sm/Sp	This study
pBbCas9^{D10A}S(RBSmut)_P_{syn}-sgRNAvls11	CJW7295	Sm/Sp	This study
pBbCas9^{D10A}S(RBSmut)_P_{syn}-sgRNAbbf03	CJW7298	Sm/Sp	This study
pBbCas9^{D10A}S(RBSmut)_P_{syn}-sgRNAbbe10	CJW7296	Sm/Sp	This study
pBbCas9^{D10A}S(RBSmut)_P_{syn}-sgRNAbbe17	CJW7297	Sm/Sp	This study
iii. Shuttle vectors expressing the nickase $Cas9^{H840A}$			
pBbCas9^{H840A}S	CJW7108	Sm/Sp	This study
pBbCas9^{H840A}S_arr2	CJW7109	Sm/Sp, Rf	This study
pBbCas9^{H840A}S_P_{syn}-sgRNA500	CJW7110	Sm/Sp	This study
pBbCas9^{H840A}S_P_{syn}-sgRNAvlsE1	CJW7128	Sm/Sp	This study
pBbCas9^{H840A}S_P_{syn}-sgRNAvlsE2	CJW7129	Sm/Sp	This study
pBbCas9^{H840A}S_P_{syn}-sgRNAvls11	CJW7246	Sm/Sp	This study
pBbCas9^{H840A}S_P_{syn}-sgRNAbbf03	CJW7249	Sm/Sp	This study
pBbCas9^{H840A}S_P_{syn}-sgRNAbbe10	CJW7247	Sm/Sp	This study
pBbCas9^{H840A}S_P_{syn}-sgRNAbbe17	CJW7248	Sm/Sp	This study
pBbCas9^{H840A}S(RBSmut)	CJW7155	Sm/Sp	This study
pBbCas9^{H840A}S(RBSmut)_arr2	CJW7166	Sm/Sp, Rf	This study
pBbCas9^{H840A}S(RBSmut)_P_{syn}-sgRNA500	CJW7157	Sm/Sp	This study
pBbCas9^{H840A}S(RBSmut)_P_{syn}-sgRNAvlsE1	CJW7158	Sm/Sp	This study
pBbCas9^{H840A}S(RBSmut)_P_{syn}-sgRNAvlsE2	CJW7159	Sm/Sp	This study
pBbCas9^{H840A}S(RBSmut)_P_{syn}-sgRNAvls11	CJW7250	Sm/Sp	This study
pBbCas9^{H840A}S(RBSmut)_P_{syn}-sgRNAbbf03	CJW7253	Sm/Sp	This study
pBbCas9^{H840A}S(RBSmut)_P_{syn}-sgRNAbbe10	CJW7251	Sm/Sp	This study
pBbCas9^{H840A}S(RBSmut)_P_{syn}-sgRNAbbe17	CJW7252	Sm/Sp	This study
pBbCas9^{H840A}S(-10TC)	CJW7160	Sm/Sp	This study

pBbCas9^{H840A}S(-10TC)_arr2	CJW7161	Sm/Sp, Rf	This study
pBbCas9^{H840A}S(-10TC)_P_{syn}-sgRNA500	CJW7162	Sm/Sp	This study
pBbCas9^{H840A}S(-10TC)_P_{syn}-sgRNAvlsE1	CJW7163	Sm/Sp	This study
pBbCas9^{H840A}S(-10TC)_P_{syn}-sgRNAvlsE2	CJW7164	Sm/Sp	This study
pBbCas9^{H840A}S(-10TC)_P_{syn}-sgRNAvls11	CJW7254	Sm/Sp	This study
pBbCas9^{H840A}S(-10TC)_P_{syn}-sgRNAbbe17	CJW7255	Sm/Sp	This study
iv. Shuttle vectors expressing wild-type Cas9			
pBbCas9S(RBSmut)	CJW7283	Sm/Sp	This study
pBbCas9S(RBSmut)_arr2	CJW7284	Sm/Sp, Rf	This study
pBbCas9S(RBSmut)_P_{syn}-sgRNA500	CJW7285	Sm/Sp	This study
pBbCas9S(RBSmut)_P_{syn}-sgRNAvlsE1	CJW7286	Sm/Sp	This study
pBbCas9S(RBSmut)_P_{syn}-sgRNAvls11	CJW7278	Sm/Sp	This study
pBbCas9S(RBSmut)_P_{syn}-sgRNAbbf03	CJW7279	Sm/Sp	This study
pBbCas9S(RBSmut)_P_{syn}-sgRNAbbe10	CJW7288	Sm/Sp	This study
pBbCas9S(RBSmut)_P_{syn}-sgRNAbbe17	CJW7289	Sm/Sp	This study

[a]Naming of the *E. coli/B. burgdorferi* shuttle vectors follows the nomenclature established and described in detail in [51]. Of note, Cas9 variant expression is driven either by the IPTG-inducible P_{pQE30} promoter or by its mutant versions in which the -10 region of the promoter (-10TC) or the ribosome binding site (RBSmut) were mutated to reduce basal Cas9 expression; [b]When requesting a plasmid from the Jacobs-Wagner lab, please include the CJW strain number alongside the plasmid name. For constructs previously published in [51], a CJW strain number is not provided, as the plasmids are available from Addgene. Please refer to the original publication for the Addgene catalog numbers; [c]Sm/Sp, streptomycin/spectinomycin resistance conferred by the *aadA* gene; Rf, rifampin resistance conferred by the *arr2* gene; Gm, gentamicin resistance conferred by the *aacC1* gene.

Targeting Cas9 activity to endogenous *B. burgdorferi* plasmids causes plasmid loss

We electroporated the shuttle vectors described above into strain K2. As controls, we used shuttle vectors lacking the sgRNA cassette and shuttle vectors expressing dCas9 rather than Cas9^{WT} (Table 2). For each construct, we plated the electroporated cells after about three generations, grew a small number of the resulting clones, and determined their endogenous plasmid content by multiplex PCR, as previously described [61]. We found that all clones that had received a shuttle vector expressing Cas9^{WT} and the *vlsE*-targeting sgRNAvlsE1 had lost the *vlsE*-carrying plasmid lp28-1 (Table 3, Fig. 3). This was not due to widespread loss of lp28-1 from the parental strain, as clones obtained from electroporation of a shuttle vector expressing Cas9^{WT} but no sgRNA retained their lp28-1 plasmid (Table 3, Fig. 3). Similarly, electroporation of shuttle vectors encoding catalytically inactive dCas9, either alone or alongside sgRNAvlsE1 or sgRNAvlsE2, did not cause widespread lp28-1 loss (Table 3). The loss of

lp28-1 occurred in spite of the presence of the adjacent homologous *vls2 – vls16* sequences that are used as donors for the generation of variant *vlsE* sequences during mammalian infection. There was also extensive plasmid loss when we targeted Cas9^{WT} to two other sites on lp28-1: the silent cassette *vls11* or to the non-*vls* gene *bbf03* (Table 3, Fig. 3). Therefore, Cas9^{WT}-mediated lp28-1 loss requires both Cas9 activity and targeting of this activity to the lp28-1 plasmid by a sgRNA regardless of where the DNA cut occurs. This effect was not limited to lp28-1, as targeting Cas9^{WT} to genes *bbe10* or *bbe17* on endogenous plasmid lp25 resulted in loss of plasmid lp25 but not of lp28-1 (Table 3). All other endogenous *B. burgdorferi* plasmids were retained in almost all clones analyzed (Table 3). As with lp28-1, the loss of lp25 was dependent on Cas9 activity and the expression of a lp25-specific sgRNA, as expressing Cas9^{WT} alone, or targeting dCas9 to lp25 did not affect lp25 retention (Table 3). We note that the transformants were selected and grown in the absence of Cas9 expression by IPTG induction. Presumably, the previously documented low but detectable basal expression of Cas9 from this system [51] generates enough activity to induce plasmid loss.

Figure 3. Targeting Cas9 activity to lp28-1 causes the loss of this plasmid from the cell population. Cells of *B. burgdorferi* strain K2 were electroporated with shuttle vectors expressing Cas9^{WT} and the indicated sgRNAs. Four clones obtained from each transformation were analyzed by multiplex PCR for the presence or absence of *B. burgdorferi* endogenous plasmids. The PCR reactions were grouped into six sets. The endogenous plasmids corresponding to each of the bands are listed on the right. Signal intensity was scaled to ensure that all positive bands could be seen. As a result, the intensities of some bands are saturated.

194

Table 3. Endogenous plasmid retention in individual *B. burgdorferi* clones after electroporation of Cas9/sgRNA vectors, as detected by multiplex PCR[a]

Cas9 version	Endogenous *B. burgdorferi* plasmid targeted	sgRNA	Clones analyzed	Plasmid retention (detected count / expected count for full retention)[b]	
				Targeted plasmid (lp28-1 or lp25)	All other tested plasmids combined
$Cas9^{WT}$	None	None	4	N/A[c]	72/72
	lp28-1	vlsE1	4	0/4	68/68
		vls11	4	0/4	68/68
		bbf03	4	0/4	68/68
	lp25	bbe10	4	0/4	67/68
		bbe17	4	0/4	68/68
dCas9	None	None	4	N/A	72/72
	lp28-1	vlsE1	4	4/4	68/68
		vlsE2	4	3/4	67/68
		vls11	4	4/4	68/68
		bbf03	4	4/4	68/68
	lp25	bbe10	4	4/4	68/68
		bbe17	4	4/4	68/68
$Cas9^{D10A}$	None	None	4	N/A	70/72
	lp28-1	vlsE1	4	0/4	68/68
		vlsE2	4	0/4	68/68
		vls11	4	0/4	68/68
		bbf03	4	3/4	68/68
	lp25	bbe10	4	0/4	68/68
		bbe17	4	4/4	68/68
$Cas9^{H840A}$	None	None	8	N/A	143/144
	lp28-1	vlsE1	16	0/16	272/272
		vlsE2	16	0/16	272/272
		vls11	4	0/4	68/68
		bbf03	4	2/4	68/68
	lp25	bbe10	4	0/4	68/68
		bbe17	4	4/4	68/68

[a]Data was aggregated based on the Cas9 version and the sgRNA expressed by the shuttle vector. Transformed strains carrying the same sgRNA but expressing different basal levels of the Cas9 variant were analyzed together. Plasmid detection was achieved by multiplex PCR [61]; [b]Data compares the number of endogenous plasmids detected in the analyzed clones with the expected number of endogenous plasmids if they had all been retained. All plasmid counts are combined for the non-targeted plasmids. A total of 18 non-targeted plasmids were assayed for each clone obtained by transformation with a shuttle vector lacking a sgRNA. A total of 17 non-targeted plasmids were assayed for each clone obtained by transformation with a shuttle vector expressing a sgRNA; [c]N/A, not applicable.

195

Performing multiplex PCR assays on individual clones is relatively labor-intensive. Additionally, if Cas9^{WT}-mediated plasmid loss is not 100% effective, the fraction of cells that still retain the targeted plasmid might be below detection. To avoid these drawbacks, we quantified endogenous plasmid retention by plating electroporated *B. burgdorferi* populations under differential antibiotic selection. In these plating assays, we used strain K2, in which retention of plasmid lp25 allows colony formation in the presence of kanamycin. Additionally, we derived strain CJW_Bb471 from strain K2 by inserting a gentamicin resistance cassette in its lp28-1 plasmid. This genetic modification does not interfere with *B. burgdorferi*'s ability to infect mice or be acquired by ticks [34]. Plating CJW_Bb471 transformants in the presence of kanamycin assays retention of lp25, while plating in the presence of gentamicin examines retention of lp28-1. In both cases, acquisition of streptomycin resistance indicates successful delivery of the Cas9-expressing shuttle vector. The number of streptomycin-resistant transformants detected in these experiments varied significantly both within an experiment and between experiments (Fig. S1A), as did transformation frequencies, as measured in one of the experiments (Fig. S1B). Despite these limitations, we could detect the following trends (see Tables 4 and 5 and Fig. 4). First, targeting Cas9^{WT} to either lp25 or lp28-1 did not result in the recovery of transformants retaining the targeted plasmid. Second, targeted dCas9 did not destabilize the targeted plasmids. Third, all Cas9 versions failed to destabilize lp25 or lp28-1 in the absence of a targeting sgRNA. Based on the number of clones that received the Cas9-expressing shuttle vector in each of the electroporations, we calculated the lowest frequency at which we could detect clones retaining the targeted endogenous plasmids (Fig. S1). These experimental limits of detection of plasmid retention within the transformed cell populations also varied significantly from electroporation to electroporation. The lowest limit of detection was around 10^{-3} (Fig. S1C). This value indicates that DSB repair mechanisms that occur less frequently than in one cell out of 1,000 cells could not be detected in our assay.

Figure 4. Summary of the *B. burgdorferi* transformation results. Graph compiling the plasmid retention values measured in experiment 3 described in Tables 4 and 5. Plasmid retention was calculated by dividing the concentration of cells that received the Cas9/sgRNA-expressing shuttle vector and retained the targeted plasmid by the concentration of cells that received the shuttle vector for any given electroporation. Experimental samples were grouped as follows. The "No sgRNA" group combines transformations of shuttle vectors encoding each of the four Cas9 versions ($Cas9^{WT}$, $Cas9^{D10A}$, $Cas9^{H840A}$, and dCas9) but no sgRNA. These transformations were plated under either kanamycin or gentamicin selection to assess retention of lp25 or lp28-1, respectively. All other transformations are grouped based on the version of Cas9 expressed from the shuttle vector and combine lp28-1 and lp25-targeting constructs.

230

Table 4. Linear plasmid 25 (lp25) retention in *B. burgdorferi* following Cas9 targeting, as detected by plating.

Host strain (marked endogenous plasmid)	Cas9 version	sgRNA	Transformants detected by plating (CFU/mL)[a]	
			CFU/mL (selection for shuttle vector and endogenous plasmid)	CFU/mL (selection for shuttle vector alone)
K2 (lp25) Experiment 1	$Cas9^{WT}$	bbe10	0	910
		bbe17	0	500
	dCas9	bbe10	610	760
		bbe17	530	450
	$Cas9^{D10A}$	bbe10	118	810
		bbe17	370	530
	$Cas9^{H840A}$	bbe10	310	770
		bbe17	520	430
CJW_Bb471 (lp25) Experiment 3[b]	$Cas9^{WT}$	None	10	6.9
		bbe10	0	12.3
		bbe17	0	17.7
	dCas9	None	22.3	37.7
		bbe10	145	127.5
		bbe17	102.5	67.5
	$Cas9^{D10A}$	None	82.5	107.5
		bbe17	202.5	160
	$Cas9^{H840A}$	None	47.7	34.6
		bbe10	0	1.5
		bbe17	1360	1380

[a]Different volumes of transformant cultures were plated under streptomycin selection (which selects for the shuttle vector), or streptomycin + kanamycin selection (which selects for lp25). Colonies were counted after 2-3 weeks and the resulting count was used to calculate the concentration of selectable cells in the parental population of transformants, expressed as colony forming units (CFU) per mL; [b]Retention of both lp25 and lp28-1 was assayed in experiment 3 following electroporation of the indicated constructs. For this reason, results from this experiment are presented in both Tables 4 and 5.

231

232

Table 5. Linear plasmid 28-1 (lp28-1) retention in *B. burgdorferi* following Cas9 targeting, as detected by plating.

Host strain (marked endogenous plasmid)	Cas9 version	sgRNA	Transformants detected by plating (CFU/mL)[a]	
			CFU/mL (selection for shuttle vector and endogenous plasmid)	CFU/mL (selection for shuttle vector alone)
CJW_Bb471 (lp28-1) Experiment 2	$Cas9^{WT}$	None	6.9	16.2
		vlsE1	0	5.4
	dCas9	None	2.3	4.6
		vlsE1	6.9	4.6
		vlsE2	3.1	9.2
	$Cas9^{D10A}$	None	2.3	1.5
		vlsE1	1.5	5.4
		vlsE2	3.1	4.6
	$Cas9^{H840A}$	None	0.8	3.8
		vlsE1	0	14.6
		vlsE2	0	5.4
CJW_Bb471 (lp28-1) Experiment 3[b]	$Cas9^{WT}$	None	13.8	6.9
		vlsE1	0	380
		vls11	0	16.1
		bbf03	0	29.2
	dCas9	None	46.9	37.7
		vlsE1	35.4	39.2
		vlsE2	7.7	9.2
		vls11	29.2	16.1
		bbf03	11.5	5.4
	$Cas9^{D10A}$	None	95	107.5
		vlsE2	0	7.7
		vls11	0	0.8
		bbf03	3.1	2.3
	$Cas9^{H840A}$	None	51.5	34.6
		vlsE1	64.6	700
		vlsE2	58.5	270
		vls11	11.5	35
		bbf03	2.3	0.8

[a]Different volumes of transformant cultures were plated under streptomycin selection (which selects for the shuttle vector), or streptomycin + gentamicin (which selects for lp28-1). Colonies were counted and the resulting count was used to calculate the concentration of selectable cells in the parental population of transformants, expressed as colony forming units (CFU) per mL; [b]Retention of both lp25 and lp28-1 was assayed in experiment 3 following electroporation of the indicated constructs. For this reason, results from this experiment are presented in both Tables 4 and 5.

233

Destabilizing effects of Cas9 nickases on *B. burgdorferi* endogenous plasmids

While Cas9^{WT} robustly and specifically induced plasmid loss when targeted to lp25 or lp28-1 (Tables 3-5, Fig. 4), the nickases Cas9^{D10A} and Cas9^{H840A} exhibited more heterogeneous behaviors. When analyzing by multiplex PCR the clones isolated in the absence of selection for the targeted plasmid, we found that targeting the nickases to the *vls* region of lp28-1 or the *bbe10* locus of lp25 was more efficient at causing plasmid loss than targeting the nickases to the *bbf03* locus of lp28-1 or the *bbe17* locus of lp25 (Table 3). We noticed a similar trend when we selected the transformants for the targeted plasmid (Tables 4 and 5, Fig. 4). These differences could be due to distinct targeting efficiencies by the sgRNAs or could reflect varied efficiencies in repairing SSBs induced at the sgRNA-targeted location.

DISCUSSION

We previously showed that targeting dCas9 to selected *B. burgdorferi* genes causes specific and efficient downregulation of gene expression, allowing for relatively easy and fast strain generation and phenotypic investigation [51]. In this study, we show that targeting Cas9^{WT} or its nickase variants to plasmid-encoded loci results in plasmid loss, though to a varying degree (Tables 3-5 and Fig. 4). In the case of Cas9^{WT}, plasmid loss was very efficient, indicating that repair of double-stranded DNA breaks generated in this manner occurs below the detection limit of our assay, i.e., less than one in 10^3 cells retained the targeted endogenous plasmid, based on the highest number of transformants recovered after Cas9 shuttle vector electroporation (Fig. S1A,C). The nickases Cas9^{D10A} and Cas9^{H840A} also cause significant plasmid loss. Presumably, a considerable fraction of nicked plasmids undergo degradation before DNA repair factors can be recruited to the site of the SSBs. Alternatively, repair of DNA lesions may be less efficient in *B. burgdorferi* compared to other bacteria, as several DNA repair factors (e.g., *mutH, lexA, ruvC, sbcB, recFOR, recX*) are absent from the *B. burgdorferi* genome [6, 62]. When

considering the limit of detection of our assay (Fig. S1C), our results suggest that the efficiency of DSB repairs in *B. burgdorferi* is at least below 10^{-3} even when donor sequences are present as in the case of *vlsE* and *vls11*. Further work will be required to gain better insight into the mechanisms employed by *B. burgdorferi* to repair DNA lesions.

Importantly, our work shows that targeting $Cas9^{WT}$ to an endogenous *B. burgdorferi* plasmid is an easy and efficient method to displace the plasmid. The Cas9 nickases can also be used to achieve this outcome, but they are less effective. Our Cas9-based approach provides an alternative to the previously developed method that displaces endogenous plasmids through introduction of shuttle vectors belonging to the same plasmid compatibility class [33-39]. Both methods yield clones in which the targeted endogenous plasmid is replaced by a shuttle vector that carries an antibiotic resistance marker. The Cas9-based method, however, does not require prior knowledge of the targeted plasmid's replication and segregation locus [7, 33-39, 63, 64], and involves only an easy cloning step to insert the sgRNA sequence into the Cas9 shuttle vector. Additionally, as Cas9 activity can be simultaneously targeted to multiple locations in the genome by co-expression of relevant sgRNAs [50], simultaneous removal of multiple plasmids from a *B. burgdorferi* strain should be achievable via a single transformation.

While the degree of genome segmentation in Borreliaceae is the highest among the known bacteria, other bacteria have segmented genomes that can include circular and linear chromosomes, chromids, megaplasmids, as well as smaller plasmids [5]. Plasmids often encode virulence factors or antibiotic resistance genes and are stably maintained by highly effective plasmid segregation mechanisms that ensure faithful inheritance by daughter cells over generations [65]. The study of plasmid-encoded functions in bacteria other than the Lyme disease spirochetes can therefore be facilitated by

implementation of a Cas9-mediated plasmid curation protocol. Translation of this approach across bacterial phyla is likely feasible, as demonstrated by the successful broad implementation of CRISPR-based methods of gene regulation [66].

ACKNOWLEDGEMENTS

We thank Dr. Patricia Rosa for sharing strain K2 and plasmid p28-1::flgBp-aacC1, the members of the Jacobs-Wagner lab for critical reading of the manuscript, and Dr. George Chaconas for valuable discussions. C.N.T. was supported in part by an American Heart Association postdoctoral fellowship (award number 18POST33990330). C.J.-W. is a Howard Hughes Medical Institute Investigator. Y.N. was supported by the Bay Area Lyme Foundation and the Brandeis University Provost's Research Fund. J.E.H. was supported by NIH grant R35 GM127029. The funders had no role in study design, data collection, analysis, and interpretation, decision to submit the work for publication, or preparation of the manuscript.

AUTHOR CONTRIBUTIONS

C.N.T. performed and analyzed all *B. burgdorferi* experiments except for the next generation sequencing analyses. Y.N. designed the sgRNAs and performed the sequencing analysis. C.J.-W. and J.E.H supervised the work. C.N.T and C.J.-W. wrote the paper with input from J.E.H. and Y.N.

MATERIALS and METHODS

E. coli strains and growth conditions

E. coli host strain NEB 5-alpha F' I^q (New England Biolabs) was exclusively used to generate, store, and amplify the *E. coli*/*B. burgdorferi* shuttle vectors listed in Table 2. The resulting strains were grown on

LB agar plates or in Super Broth (35 g/L bacto-tryptone, 20 g/L yeast extract, 5 g/L NaCl, and 6 mM NaOH) liquid medium with shaking at 30°C [67]. Transformation was achieved by heat shock followed by recovery in SOC medium (New England Biolabs) for 1h at 30°C with shaking. Antibiotic selection was achieved using spectinomycin at 50 μg/mL or rifampin at 25 μg/mL in liquid culture or 50 μg/mL in plates.

B. burgdorferi strains and growth conditions

Previously described *B. burgdorferi* strain B31-A3-68-Δ*bbe02*::P_{flgB}-*aphI*, also known as K2, is an infectious, highly transformable derivative of the type strain B31 [59]. To derive strain CJW_Bb471 from K2, pseudogene *bbf29* of plasmid lp28-1 was disrupted by insertion of a gentamicin resistance cassette. Strains K2 and CJW_Bb471 contain 18 of the 21 endogenous plasmids of parental strain B31; they both lack endogenous plasmids cp9, lp5, and lp56 [6, 59]. To generate strain CJW_Bb471, 75 μg of plasmid p28-1::flgBp-aacC1 [34] were digested with *Age*I-HF (New England Biolabs), ethanol precipitated [68], resuspended in 25 μL water, and electroporated into a 100 μL aliquot of K2 electrocompetent cells. Electroporated cells were immediately transferred to 6 mL complete Barbour-Stoenner-Kelly (BSK)-II medium and allowed to recover overnight. The following day, cells were plated in semisolid BSK-agarose medium under kanamycin and gentamicin selection. A clone was grown and confirmed to have correct insertion of the gentamicin resistance cassette into lp28-1 and to contain all the endogenous plasmids of the parental strain.

B. burgdorferi strains were grown in complete BSK-II medium at 34°C in a humidified 5% CO_2 incubator [69-71]. BSK-II medium contained 50 g/L Bovine Serum Albumin, Universal Grade (Millipore), 9.7 g/L CMRL-1066 (US Biological), 5 g/L Neopeptone (Difco), 2 g/L Yeastolate (Difco),

6 g/L HEPES (Millipore), 5 g/L glucose (Sigma-Aldrich), 2.2 g/L sodium bicarbonate (Sigma-Aldrich), 0.8 g/L sodium pyruvate (Sigma-Aldrich), 0.7 g/L sodium citrate (Fisher Scientific), 0.4 g/L N-acetylglucosamine (Sigma-Aldrich), 60 mL/L heat-inactivated rabbit serum (Gibco), and had a pH of 7.6. For plating in semisolid BSK-agarose medium [51], each 10-cm plate was seeded with up to 1 mL *B. burgdorferi* culture. BSK-agarose plating medium was made by mixing two volumes of 1.7 % agarose in water, melted and pre-equilibrated at 55°C with three volumes of BSK-1.5 medium, also briefly (for less than 5 min) pre-equilibrated at 55 °C and containing appropriate amounts of antibiotics. Then, 25 mL of the BSK-agarose mix was added to each seeded plate, which was then gently swirled and allowed to solidify for ~30 min at room temperature in a biosafety cabinet. The plates were then transferred to a humidified 5% CO_2 incubator kept at 34 °C. BSK-1.5 medium contained 69.4 g/L BSA, 12.7 g/L CMRL-1066, 6.9 g/L Neopeptone, 3.5 g/L Yeastolate, 8.3 g/L HEPES, 6.9 g/L glucose, 6.4 g/L sodium bicarbonate, 1.1 g/L sodium pyruvate, 1.0 g/L sodium citrate, 0.6 g/L N-acetylglucosamine, 40 mL/L heat-inactivated rabbit serum, and had a pH of 7.5. Antibiotics were used at the following concentrations: streptomycin at 100 μg/mL, gentamicin at 40 μg/mL, and kanamycin at 200 μg/mL [72-74]. Unless otherwise indicated, *B. burgdorferi* cultures were maintained in exponential growth by diluting cultures into fresh medium before cultures densities reached ~5 x 10^7 cells/mL. Cell density of cultures was determined by direct counting under darkfield illumination using disposable hemocytometers, as previously described [67].

B. burgdorferi **transformation, clone isolation, and characterization**

Electrocompetent cells were generated as previously described [75] and stored as single use 50 or 100 μL aliquots at -80°C. For shuttle vector transformations, 30 or 50 μg of plasmid eluted in water were electroporated (2.5 kV, 25 μF, 200 Ω, 2 mm gap cuvette) into 50 μL aliquots of competent cells.

Electroporated cells were immediately transferred to 6 mL BSK-II and allowed to recover overnight. The next day, 100, 300, and 900 µL aliquots of the culture were each plated in semisolid BSK-agarose under selection. The remaining culture was diluted 6-fold in BSK-II and selected in liquid culture with appropriate antibiotics. Once transformants were observed as motile spirochetes, the liquid cultures were plated for clone isolation. Agarose plugs containing individual colonies were used to inoculate 6 mL BSK-II cultures. After 3 days, 500 to 1000 µL of each clonal culture was removed and pelleted at 10,000 x g for 10 min, the cells were resuspended and lysed in 50-100 µL water, and the resulting solution was used to perform multiplex PCR using primer pairs specific for each endogenous plasmid of strain B31 [61] and the DreamTaq Green DNA Polymerase (Thermo Scientific). For genomic DNA extraction, ~14 mL cultures were grown to ~10^8 cells/mL and then pelleted at 4,300 x g for 10 min at room temperature in a Beckman Coulter X-14R centrifuge equipped with a swinging bucket rotor. The media was removed and the pellet was processed for DNA extraction using QIAGEN's DNeasy Blood & Tissue Kit protocol for Gram-negative bacteria. Final elution was carried out in 10 mM Tris-HCl, 0.1 mM EDTA, pH 9.0.

Generation of *E. coli*/*B. burgdorferi* shuttle vectors for Cas9 and sgRNA expression

Table 2 lists the *E. coli/B. burgdorferi* shuttle vectors used or generated in this study. They were based on the previously described *B. burgdorferi* CRISPR interference platform [51]. The shuttle vectors express one of the following Cas9 versions: wild-type Cas9, the nickases $Cas9^{D10A}$ or $Cas9^{H840A}$, or the catalytically inactive dCas9 that carries both the D10A and H840A mutations. To revert the D10A mutation, site-directed mutagenesis was performed on appropriate template plasmids using Agilent's Quick Change Lightning Site-Directed Mutagenesis kit and primers NT651 and NT652. To revert the H840A mutation, site-directed mutagenesis was performed on appropriate template plasmids using primers NT749 and NT750. To generate plasmids with decreased basal expression of Cas9 proteins [51],

site-directed mutagenesis was performed on appropriate plasmid templates using primers NT669 and NT670, which generated a weakened ribosomal binding site ("RBSmut" constructs), or primers NT677 and NT678, which introduced a mutation in the -10 region of the Cas9 promoter ("-10TC" constructs). Expression cassettes for the sgRNAs were moved among plasmids using restriction endonucleases *Asc*I and *Eag*I. To generate sgRNA expression cassettes, *Sap*I-digested Psyn-sgRNA500-containing plasmids were ligated with annealed primer pairs, as follows: primers NT657 and NT658 generated sgRNAvlsE1; NT660 and NT661 generated sgRNAvlsE2; NT721 and NT722 generated sgRNAvls11; NT723 and NT724 generated sgRNAbbe10; NT725 and NT726 generated sgRNAbbe17; and NT727 and NT728 generated sgRNAbbf03. Primer annealing was achieved by mixing 10 µL volumes of each primer at 5 µM concentration, then cycling the mix five times between 30 s at 95°C and 30 s at 55°C, followed by cooling to room temperature. Nucleotide sequences of primers used to generate the *E. coli*/*B. burgdorferi* shuttle vectors in this study are given in Table 6.

Table 6. Oligonucleotide primers used in this study

Name	Sequence (5' to 3')
NT651	GGATAAGAAATACTCAATAGGCTTAGATATCGGCACAAATAGCGTCGGATGGG
NT652	CCCATCCGACGCTATTTGTGCCGATATCTAAGCCTATTGAGTATTTCTTATCC
NT657	AGTGCTACAGGGGAGAATAATAA
NT658	AACTTATTATTCTCCCCTGTAGC
NT660	AGTGGATGGAGAGAAGCCTGAGG
NT661	AACCCTCAGGCTTCTCTCCATCC
NT669	GATAACAATTTCACACAGAATTCATTAAAGAAGAGAAATTACATATGGATAAGAAATAC
NT670	GTATTTCTTATCCATATGTAATTTCTCTTCTTTAATGAATTCTGTGTGAAATTGTTATC
NT677	GCTTTGTGAGCGGATAACAATTATAACAGATTCAATTGTGAGCGGATAACAATTTCACAC
NT678	GTGTGAAATTGTTATCCGCTCACAATTGAATCTGTTATAATTGTTATCCGCTCACAAAGC
NT721	AGTGCTGTTAGTGCTGGTTAGTG
NT722	AACCACTAACCAGCACTAACAGC
NT723	AGTAGGGGGAAGACAATTTACTT
NT724	AACAAGTAAATTGTCTTCCCCCT
NT725	AGTAATATTCTTTCAGGGTAAGC
NT726	AACGCTTACCCTGAAAGAATATT
NT727	AGTAGAGTTTCTACGATTGAGTA
NT728	AACTACTCAATCGTAGAAACTCT
NT749	TAATCGTTTAAGTGATTATGATGTCGATCATATTGTTCCACAAAGTTTCCTTAAAGACG

NT750	CGTCTTTAAGGAAACTTTGTGGAACAATATGATCGACATCATAATCACTTAAACGATTA
YN-LI_266	GTATTTGTTGTTAAGTAGATAGGAATATTTCGG
YN-LI_267	CGTGTCCATACACTTAATTAAATCACTTATTC

DNA sequence analysis

To determine the sequence of the *vls* locus of *B. burgdorferi* strain K2, the 10910 base pair region encompassing *vlsE* and silent cassettes *vls2-vls16* was amplified using Platinum™ SuperFi™ DNA Polymerase (Thermo Fisher Scientific) and primers YN-LI_266 and YN-LI_267 (Table 6) and then sequenced with a SMRT Cell™ using 10-h data collection (Pacific Biosciences). The resulting reads were subjected to read-of-insert (ROI) analysis using SMRT Link v6.0.0 (Pacific Biosciences), followed by multiple sequence alignment, to obtain the final consensus sequence.

Data and material availability

B. burgdorferi strains and *E. coli*/*B. burgdorferi* shuttle vectors generated in this study (Table 2) are available upon request from Christine Jacobs-Wagner.

REFERENCES

1. Kugeler KJ, Schwartz AM, Delorey MJ, Mead PS, Hinckley AF. Estimating the frequency of Lyme disease diagnoses, United States, 2010-2018. Emerg Infect Dis. 2021;27(2):616-9. doi: 10.3201/eid2702.202731. PubMed PMID: 33496229; PubMed Central PMCID: PMCPMC7853543.
2. Mead PS. Epidemiology of Lyme disease. Infect Dis Clin North Am. 2015;29(2):187-210. doi: 10.1016/j.idc.2015.02.010. PubMed PMID: 25999219.
3. Steere AC, Strle F, Wormser GP, Hu LT, Branda JA, Hovius JW, et al. Lyme borreliosis. Nat Rev Dis Primers. 2016;2:16090. doi: 10.1038/nrdp.2016.90. PubMed PMID: 27976670.
4. Radolf JD, Caimano MJ, Stevenson B, Hu LT. Of ticks, mice and men: understanding the dual-host lifestyle of Lyme disease spirochaetes. Nat Rev Microbiol. 2012;10(2):87-99. doi: 10.1038/nrmicro2714. PubMed PMID: 22230951; PubMed Central PMCID: PMC3313462.
5. diCenzo GC, Finan TM. The divided bacterial genome: structure, function, and evolution. Microbiol Mol Biol Rev. 2017;81(3). doi: 10.1128/MMBR.00019-17. PubMed PMID: 28794225; PubMed Central PMCID: PMCPMC5584315.
6. Fraser CM, Casjens S, Huang WM, Sutton GG, Clayton R, Lathigra R, et al. Genomic sequence of a Lyme disease spirochaete, *Borrelia burgdorferi*. Nature. 1997;390(6660):580-6. doi: 10.1038/37551. PubMed PMID: 9403685.
7. Casjens S, Palmer N, van Vugt R, Huang WM, Stevenson B, Rosa P, et al. A bacterial genome in flux: the twelve linear and nine circular extrachromosomal DNAs in an infectious isolate of the

Lyme disease spirochete *Borrelia burgdorferi*. Mol Microbiol. 2000;35(3):490-516. PubMed PMID: 10672174.

8. Kitten T, Barbour AG. The relapsing fever agent *Borrelia hermsii* has multiple copies of its chromosome and linear plasmids. Genetics. 1992;132(2):311-24. PubMed PMID: 1427031; PubMed Central PMCID: PMC1205138.
9. Takacs CN, Wachter J, Xiang Y, Karaboja X, Ren Z, Scott M, et al. Polyploidy, regular patterning of genome copies, and unusual control of DNA partitioning in the Lyme disease spirochete. bioRxiv. 2022. doi: 10.1101/2022.07.05.498848.
10. Schwartz I, Margos G, Casjens SR, Qiu WG, Eggers CH. Multipartite genome of Lyme disease *Borrelia*: structure, variation and prophages. Curr Issues Mol Biol. 2021;42:409-54. doi: 10.21775/cimb.042.409. PubMed PMID: 33328355.
11. Chaconas G, Castellanos M, Verhey TB. Changing of the guard: how the Lyme disease spirochete subverts the host immune response. J Biol Chem. 2020;295(2):301-13. doi: 10.1074/jbc.REV119.008583. PubMed PMID: 31753921; PubMed Central PMCID: PMCPMC6956529.
12. Anderson C, Brissette CA. The brilliance of *Borrelia*: mechanisms of host immuneevasion by Lyme disease-causing spirochetes. Pathogens. 2021;10(3). doi: 10.3390/pathogens10030281. PubMed PMID: 33801255; PubMed Central PMCID: PMCPMC8001052.
13. Coburn J, Garcia B, Hu LT, Jewett MW, Kraiczy P, Norris SJ, et al. Lyme disease pathogenesis. Curr Issues Mol Biol. 2021;42:473-518. doi: 10.21775/cimb.042.473. PubMed PMID: 33353871; PubMed Central PMCID: PMCPMC8046170.
14. Skare JT, Garcia BL. Complement evasion by Lyme disease spirochetes. Trends Microbiol. 2020;28(11):889-99. doi: 10.1016/j.tim.2020.05.004. PubMed PMID: 32482556; PubMed Central PMCID: PMCPMC7572514.
15. Antonara S, Ristow L, Coburn J. Adhesion mechanisms of *Borrelia burgdorferi*. Adv Exp Med Biol. 2011;715:35-49. doi: 10.1007/978-94-007-0940-9_3. PubMed PMID: 21557056; PubMed Central PMCID: PMCPMC4521209.
16. Brissette CA, Gaultney RA. That's my story, and I'm sticking to it--an update on *B. burgdorfer*i adhesins. Front Cell Infect Microbiol. 2014;4:41. doi: 10.3389/fcimb.2014.00041. PubMed PMID: 24772392; PubMed Central PMCID: PMCPMC3982108.
17. Casjens SR, Gilcrease EB, Vujadinovic M, Mongodin EF, Luft BJ, Schutzer SE, et al. Plasmid diversity and phylogenetic consistency in the Lyme disease agent *Borrelia burgdorferi*. BMC Genomics. 2017;18(1):165. doi: 10.1186/s12864-017-3553-5. PubMed PMID: 28201991; PubMed Central PMCID: PMC5310021.
18. Brisson D, Zhou W, Jutras BL, Casjens S, Stevenson B. Distribution of cp32 prophages among Lyme disease-causing spirochetes and natural diversity of their lipoprotein-encoding *erp* loci. Appl Environ Microbiol. 2013;79(13):4115-28. doi: 10.1128/AEM.00817-13. PubMed PMID: 23624478; PubMed Central PMCID: PMCPMC3697573.
19. Eggers CH, Kimmel BJ, Bono JL, Elias AF, Rosa P, Samuels DS. Transduction by phiBB-1, a bacteriophage of *Borrelia burgdorferi*. J Bacteriol. 2001;183(16):4771-8. doi: 10.1128/JB.183.16.4771-4778.2001. PubMed PMID: 11466280; PubMed Central PMCID: PMCPMC99531.
20. Eggers CH, Samuels DS. Molecular evidence for a new bacteriophage of *Borrelia burgdorferi*. J Bacteriol. 1999;181(23):7308-13. doi: 10.1128/JB.181.23.7308-7313.1999. PubMed PMID: 10572135; PubMed Central PMCID: PMCPMC103694.

21. Byram R, Stewart PE, Rosa P. The essential nature of the ubiquitous 26-kilobase circular replicon of *Borrelia burgdorferi*. J Bacteriol. 2004;186(11):3561-9. doi: 10.1128/JB.186.11.3561-3569.2004. PubMed PMID: 15150244; PubMed Central PMCID: PMC415784.
22. Sadziene A, Rosa PA, Thompson PA, Hogan DM, Barbour AG. Antibody-resistant mutants of *Borrelia burgdorferi*: in vitro selection and characterization. J Exp Med. 1992;176(3):799-809. doi: 10.1084/jem.176.3.799. PubMed PMID: 1339462; PubMed Central PMCID: PMCPMC2119346.
23. Sadziene A, Wilske B, Ferdows MS, Barbour AG. The cryptic *ospC* gene of *Borrelia burgdorferi* B31 is located on a circular plasmid. Infect Immun. 1993;61(5):2192-5. doi: 10.1128/iai.61.5.2192-2195.1993. PubMed PMID: 8478109; PubMed Central PMCID: PMCPMC280820.
24. Casjens S, van Vugt R, Tilly K, Rosa PA, Stevenson B. Homology throughout the multiple 32-kilobase circular plasmids present in Lyme disease spirochetes. J Bacteriol. 1997;179(1):217-27. PubMed PMID: 8982001; PubMed Central PMCID: PMC178682.
25. Purser JE, Norris SJ. Correlation between plasmid content and infectivity in *Borrelia burgdorferi*. Proc Natl Acad Sci USA. 2000;97(25):13865-70. doi: 10.1073/pnas.97.25.13865. PubMed PMID: 11106398; PubMed Central PMCID: PMC17667.
26. Xu Y, Kodner C, Coleman L, Johnson RC. Correlation of plasmids with infectivity of *Borrelia burgdorferi* sensu stricto type strain B31. Infect Immun. 1996;64(9):3870-6. doi: 10.1128/iai.64.9.3870-3876.1996. PubMed PMID: 8751941; PubMed Central PMCID: PMCPMC174305.
27. Casjens SR, Di L, Akther S, Mongodin EF, Luft BJ, Schutzer SE, et al. Primordial origin and diversification of plasmids in Lyme disease agent bacteria. BMC Genomics. 2018;19(1):218. doi: 10.1186/s12864-018-4597-x. PubMed PMID: 29580205; PubMed Central PMCID: PMCPMC5870499.
28. Kneubehl AR, Krishnavajhala A, Leal SM, Replogle AJ, Kingry LC, Bermudez SE, et al. Comparative genomics of the Western Hemisphere soft tick-borne relapsing fever borreliae highlights extensive plasmid diversity. BMC Genomics. 2022;23(1):410. doi: 10.1186/s12864-022-08523-7. PubMed PMID: 35641918; PubMed Central PMCID: PMCPMC9158201.
29. Barbour AG. Plasmid analysis of *Borrelia burgdorferi*, the Lyme disease agent. J Clin Microbiol. 1988;26(3):475-8. doi: 10.1128/jcm.26.3.475-478.1988. PubMed PMID: 3356787; PubMed Central PMCID: PMCPMC266316.
30. Schwan TG, Burgdorfer W, Garon CF. Changes in infectivity and plasmid profile of the Lyme disease spirochete, *Borrelia burgdorferi*, as a result of in vitro cultivation. Infect Immun. 1988;56(8):1831-6. doi: 10.1128/iai.56.8.1831-1836.1988. PubMed PMID: 3397175; PubMed Central PMCID: PMCPMC259490.
31. Elias AF, Stewart PE, Grimm D, Caimano MJ, Eggers CH, Tilly K, et al. Clonal polymorphism of *Borrelia burgdorferi* strain B31 MI: implications for mutagenesis in an infectious strain background. Infect Immun. 2002;70(4):2139-50. PubMed PMID: 11895980; PubMed Central PMCID: PMC127854.
32. Grimm D, Elias AF, Tilly K, Rosa PA. Plasmid stability during in vitro propagation of *Borrelia burgdorferi* assessed at a clonal level. Infect Immun. 2003;71(6):3138-45. PubMed PMID: 12761092; PubMed Central PMCID: PMC155697.
33. Stewart PE, Thalken R, Bono JL, Rosa P. Isolation of a circular plasmid region sufficient for autonomous replication and transformation of infectious *Borrelia burgdorferi*. Mol Microbiol. 2001;39(3):714-21. PubMed PMID: 11169111.
34. Grimm D, Eggers CH, Caimano MJ, Tilly K, Stewart PE, Elias AF, et al. Experimental assessment of the roles of linear plasmids lp25 and lp28-1 of *Borrelia burgdorferi* throughout the infectious

cycle. Infect Immun. 2004;72(10):5938-46. doi: 10.1128/IAI.72.10.5938-5946.2004. PubMed PMID: 15385497; PubMed Central PMCID: PMC517563.

35. Stewart PE, Chaconas G, Rosa P. Conservation of plasmid maintenance functions between linear and circular plasmids in *Borrelia burgdorferi*. J Bacteriol. 2003;185(10):3202-9. PubMed PMID: 12730180; PubMed Central PMCID: PMC154063.
36. Dulebohn DP, Bestor A, Rego RO, Stewart PE, Rosa PA. *Borrelia burgdorferi* linear plasmid 38 is dispensable for completion of the mouse-tick infectious cycle. Infect Immun. 2011;79(9):3510-7. doi: 10.1128/IAI.05014-11. PubMed PMID: 21708994; PubMed Central PMCID: PMCPMC3165476.
37. Dulebohn DP, Bestor A, Rosa PA. *Borrelia burgdorferi* linear plasmid 28-3 confers a selective advantage in an experimental mouse-tick infection model. Infect Immun. 2013;81(8):2986-96. doi: 10.1128/IAI.00219-13. PubMed PMID: 23753630; PubMed Central PMCID: PMC3719586.
38. Jewett MW, Byram R, Bestor A, Tilly K, Lawrence K, Burtnick MN, et al. Genetic basis for retention of a critical virulence plasmid of *Borrelia burgdorferi*. Mol Microbiol. 2007;66(4):975-90. doi: 10.1111/j.1365-2958.2007.05969.x. PubMed PMID: 17919281; PubMed Central PMCID: PMC2229028.
39. Eggers CH, Caimano MJ, Clawson ML, Miller WG, Samuels DS, Radolf JD. Identification of loci critical for replication and compatibility of a *Borrelia burgdorferi* cp32 plasmid and use of a cp32-based shuttle vector for the expression of fluorescent reporters in the lyme disease spirochaete. Mol Microbiol. 2002;43(2):281-95. PubMed PMID: 11985709.
40. Cui L, Bikard D. Consequences of Cas9 cleavage in the chromosome of *Escherichia coli*. Nucl Acids Res. 2016;44(9):4243-51. doi: 10.1093/nar/gkw223. PubMed PMID: 27060147; PubMed Central PMCID: PMCPMC4872102.
41. Pennington JM, Rosenberg SM. Spontaneous DNA breakage in single living *Escherichia coli* cells. Nat Genet. 2007;39(6):797-802. doi: 10.1038/ng2051. PubMed PMID: 17529976; PubMed Central PMCID: PMCPMC2856310.
42. Bikard D, Hatoum-Aslan A, Mucida D, Marraffini LA. CRISPR interference can prevent natural transformation and virulence acquisition during in vivo bacterial infection. Cell Host Microbe. 2012;12(2):177-86. doi: 10.1016/j.chom.2012.06.003. PubMed PMID: 22901538.
43. Xu T, Li Y, Shi Z, Hemme CL, Li Y, Zhu Y, et al. Efficient genome editing in *Clostridium cellulolyticum* via CRISPR-Cas9 nickase. Appl Environ Microbiol. 2015;81(13):4423-31. doi: 10.1128/AEM.00873-15. PubMed PMID: 25911483; PubMed Central PMCID: PMCPMC4475897.
44. Fernandes LGV, Guaman LP, Vasconcellos SA, Heinemann MB, Picardeau M, Nascimento A. Gene silencing based on RNA-guided catalytically inactive Cas9 (dCas9): a new tool for genetic engineering in *Leptospira*. Sci Rep. 2019;9(1):1839. doi: 10.1038/s41598-018-37949-x. PubMed PMID: 30755626; PubMed Central PMCID: PMC6372684.
45. Prister LL, Xu J, Seifert HS. A double-strand break does not promote *Neisseria gonorrhoeae* pilin antigenic variation. J Bacteriol. 2019;201(13). doi: 10.1128/JB.00256-19. PubMed PMID: 30988037; PubMed Central PMCID: PMCPMC6560144.
46. Jinek M, Chylinski K, Fonfara I, Hauer M, Doudna JA, Charpentier E. A programmable dual-RNA-guided DNA endonuclease in adaptive bacterial immunity. Science. 2012;337(6096):816-21. doi: 10.1126/science.1225829. PubMed PMID: 22745249; PubMed Central PMCID: PMCPMC6286148.
47. Bolotin A, Quinquis B, Sorokin A, Ehrlich SD. Clustered regularly interspaced short palindrome repeats (CRISPRs) have spacers of extrachromosomal origin. Microbiology. 2005;151(Pt 8):2551-61. doi: 10.1099/mic.0.28048-0. PubMed PMID: 16079334.

552 48. Koonin EV, Makarova KS, Zhang F. Diversity, classification and evolution of CRISPR-Cas
553 systems. Curr Opin Microbiol. 2017;37:67-78. doi: 10.1016/j.mib.2017.05.008. PubMed PMID:
554 28605718; PubMed Central PMCID: PMCPMC5776717.
555 49. Larson MH, Gilbert LA, Wang X, Lim WA, Weissman JS, Qi LS. CRISPR interference (CRISPRi)
556 for sequence-specific control of gene expression. Nat Prot. 2013;8(11):2180-96. doi:
557 10.1038/nprot.2013.132. PubMed PMID: 24136345; PubMed Central PMCID: PMC3922765.
558 50. Qi LS, Larson MH, Gilbert LA, Doudna JA, Weissman JS, Arkin AP, et al. Repurposing CRISPR as
559 an RNA-guided platform for sequence-specific control of gene expression. Cell. 2013;152(5):1173-
560 83. doi: 10.1016/j.cell.2013.02.022. PubMed PMID: 23452860; PubMed Central PMCID:
561 PMC3664290.
562 51. Takacs CN, Scott M, Chang Y, Kloos ZA, Irnov I, Rosa PA, et al. A CRISPR interference platform
563 for selective downregulation of gene expression in *Borrelia burgdorferi*. Appl Environ Microbiol.
564 2021;87:e02519-20. doi: 10.1128/AEM.02519-20. PubMed PMID: 33257311; PubMed Central
565 PMCID: PMCPMC7851697.
566 52. Labandeira-Rey M, Skare JT. Decreased infectivity in *Borrelia burgdorferi* strain B31 is associated
567 with loss of linear plasmid 25 or 28-1. Infect Immun. 2001;69(1):446-55. doi: 10.1128/IAI.69.1.446-
568 455.2001. PubMed PMID: 11119536; PubMed Central PMCID: PMC97902.
569 53. Purser JE, Lawrenz MB, Caimano MJ, Howell JK, Radolf JD, Norris SJ. A plasmid-encoded
570 nicotinamidase (PncA) is essential for infectivity of *Borrelia burgdorferi* in a mammalian host. Mol
571 Microbiol. 2003;48(3):753-64. doi: 10.1046/j.1365-2958.2003.03452.x. PubMed PMID: 12694619.
572 54. Strother KO, de Silva A. Role of *Borrelia burgdorferi* linear plasmid 25 in infection of *Ixodes*
573 *scapularis* ticks. J Bacteriol. 2005;187(16):5776-81. doi: 10.1128/JB.187.16.5776-5781.2005.
574 PubMed PMID: 16077125; PubMed Central PMCID: PMC1196075.
575 55. Grimm D, Tilly K, Bueschel DM, Fisher MA, Policastro PF, Gherardini FC, et al. Defining plasmids
576 required by *Borrelia burgdorferi* for colonization of tick vector *Ixodes scapularis* (Acari: Ixodidae).
577 J Med Entomol. 2005;42(4):676-84. doi: 10.1093/jmedent/42.4.676. PubMed PMID: 16119559.
578 56. Strother KO, Broadwater A, De Silva A. Plasmid requirements for infection of ticks by *Borrelia*
579 *burgdorferi*. Vector Borne and Zoonotic Dis. 2005;5(3):237-45. doi: 10.1089/vbz.2005.5.237.
580 PubMed PMID: 16187892.
581 57. Zhang JR, Hardham JM, Barbour AG, Norris SJ. Antigenic variation in Lyme disease borreliae by
582 promiscuous recombination of VMP-like sequence cassettes. Cell. 1997;89(2):275-85. doi:
583 10.1016/s0092-8674(00)80206-8. PubMed PMID: 9108482.
584 58. Norris SJ. vls Antigenic variation systems of Lyme disease *Borrelia*: eluding host immunity through
585 both random, segmental gene conversion and framework heterogeneity. Microbiol Spectrum.
586 2014;2(6). doi: 10.1128/microbiolspec.MDNA3-0038-2014. PubMed PMID: 26104445; PubMed
587 Central PMCID: PMCPMC4480602.
588 59. Rego RO, Bestor A, Rosa PA. Defining the plasmid-borne restriction-modification systems of the
589 Lyme disease spirochete *Borrelia burgdorferi*. J Bacteriol. 2011;193(5):1161-71. doi:
590 10.1128/JB.01176-10. PubMed PMID: 21193609; PubMed Central PMCID: PMC3067601.
591 60. Wenger AM, Peluso P, Rowell WJ, Chang PC, Hall RJ, Concepcion GT, et al. Accurate circular
592 consensus long-read sequencing improves variant detection and assembly of a human genome. Nat
593 Biotechnol. 2019;37(10):1155-62. doi: 10.1038/s41587-019-0217-9. PubMed PMID: 31406327;
594 PubMed Central PMCID: PMCPMC6776680.
595 61. Bunikis I, Kutschan-Bunikis S, Bonde M, Bergstrom S. Multiplex PCR as a tool for validating
596 plasmid content of *Borrelia burgdorferi*. J Microbiol Methods. 2011;86(2):243-7. doi:
597 10.1016/j.mimet.2011.05.004. PubMed PMID: 21605603.

62. Hardy PO, Chaconas G. The nucleotide excision repair system of *Borrelia burgdorferi* is the sole pathway involved in repair of DNA damage by UV light. J Bacteriol. 2013;195(10):2220-31. doi: 10.1128/JB.00043-13. PubMed PMID: 23475971; PubMed Central PMCID: PMCPMC3650546.
63. Chaconas G, Norris SJ. Peaceful coexistence amongst *Borrelia* plasmids: getting by with a little help from their friends? Plasmid. 2013;70(2):161-7. doi: 10.1016/j.plasmid.2013.05.002. PubMed PMID: 23727020; PubMed Central PMCID: PMC3737319.
64. Tilly K, Checroun C, Rosa PA. Requirements for *Borrelia burgdorferi* plasmid maintenance. Plasmid. 2012;68(1):1-12. doi: 10.1016/j.plasmid.2012.01.009. PubMed PMID: 22289894; PubMed Central PMCID: PMC3367046.
65. Baxter JC, Funnell BE. Plasmid partition mechanisms. Microbiol Spectrum. 2014;2(6). doi: 10.1128/microbiolspec.PLAS-0023-2014. PubMed PMID: 26104442.
66. Call SN, Andrews LB. CRISPR-based approaches for gene regulation in non-model bacteria. Front Genome Ed. 2022;4:892304. doi: 10.3389/fgeed.2022.892304. PubMed PMID: 35813973; PubMed Central PMCID: PMCPMC9260158.
67. Takacs CN, Kloos ZA, Scott M, Rosa PA, Jacobs-Wagner C. Fluorescent proteins, promoters, and selectable markers for applications in the Lyme disease spirochete *Borrelia burgdorferi*. Appl Environ Microbiol. 2018;84(24). doi: 10.1128/AEM.01824-18. PubMed PMID: 30315081; PubMed Central PMCID: PMCPMC6275353.
68. Green MR, Sambrook J. Precipitation of DNA with ethanol. Cold Spring Harb Protoc. 2016;2016(12):1116-20. doi: 10.1101/pdb.prot093377. PubMed PMID: 27934690.
69. Barbour AG. Isolation and cultivation of Lyme disease spirochetes. Yale J Biol Med. 1984;57(4):521-5. PubMed PMID: 6393604; PubMed Central PMCID: PMC2589996.
70. Zuckert WR. Laboratory maintenance of *Borrelia burgdorferi*. Curr Prot Microbiol. 2007;Chapter 12:Unit 12C 1. doi: 10.1002/9780471729259.mc12c01s4. PubMed PMID: 18770608.
71. Jutras BL, Chenail AM, Stevenson B. Changes in bacterial growth rate govern expression of the *Borrelia burgdorferi* OspC and Erp infection-associated surface proteins. J Bacteriol. 2013;195(4):757-64. doi: 10.1128/JB.01956-12. PubMed PMID: 23222718; PubMed Central PMCID: PMC3562092.
72. Bono JL, Elias AF, Kupko JJ, 3rd, Stevenson B, Tilly K, Rosa P. Efficient targeted mutagenesis in *Borrelia burgdorferi*. J Bacteriol. 2000;182(9):2445-52. PubMed PMID: 10762244; PubMed Central PMCID: PMC111306.
73. Elias AF, Bono JL, Kupko JJ, 3rd, Stewart PE, Krum JG, Rosa PA. New antibiotic resistance cassettes suitable for genetic studies in *Borrelia burgdorferi*. J Mol Microbiol Biotechnol. 2003;6(1):29-40. doi: 10.1159/000073406. PubMed PMID: 14593251.
74. Frank KL, Bundle SF, Kresge ME, Eggers CH, Samuels DS. *aadA* confers streptomycin resistance in *Borrelia burgdorferi*. J Bacteriol. 2003;185(22):6723-7. PubMed PMID: 14594849; PubMed Central PMCID: PMC262111.
75. Tilly K, Elias AF, Bono JL, Stewart P, Rosa P. DNA exchange and insertional inactivation in spirochetes. J Mol Microbiol Biotechnol. 2000;2(4):433-42. PubMed PMID: 11075915.

Supplementary Figure 1. Transformation statistics. A. Transformation yield, defined as number of shuttle vector-transformed colony forming units (cfu) per mL culture measured by plating under streptomycin selection one day after electroporation. The experiment numbers are the same as in Tables 4 and 5 and are listed at the bottom. Recipient strains are also listed at the bottom. **B.** Plot showing the distribution of transformation frequency values measured in experiment 3 described in (A) and Tables 4 and 5. The transformation frequency is defined as the ratio of the number of cells that got transformed with the Cas9 shuttle vector to the number of cells that survived electroporation. Transformed and viable cell numbers were measured by plating the electroporated cells in the presence or absence of streptomycin. **C.** Plot showing the limit of detection of cells that retained the targeted endogenous plasmid for the individual electroporations performed in experiments 1 through 3 as described in panel (A) and Tables 4 and 5. The limit of detection values were calculated as follows. First, we counted the number of colonies obtained by plating the electroporated *B. burgdorferi* cultures under streptomycin selection and added the values we counted on the plates seeded with the 100, 300, and 900 μL cell culture volumes (1.3 mL total, also see Methods). If plates seeded with larger volumes of culture yielded too many colonies to allow an accurate count, the number of colony-forming cells in 1.3 mL culture was estimated from the number of colonies counted on plates seeded with the lesser culture volume(s). The limit of detection value was then calculated as the inverse of the number of colonies obtained from plating 1.3 mL electroporated culture. Labels are as in (A).

Figure 1

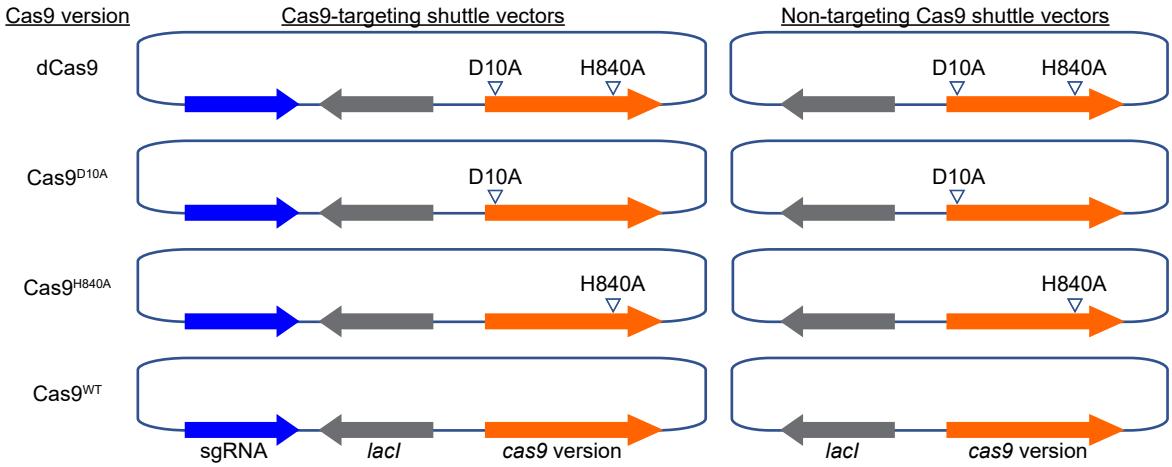

Figure 2

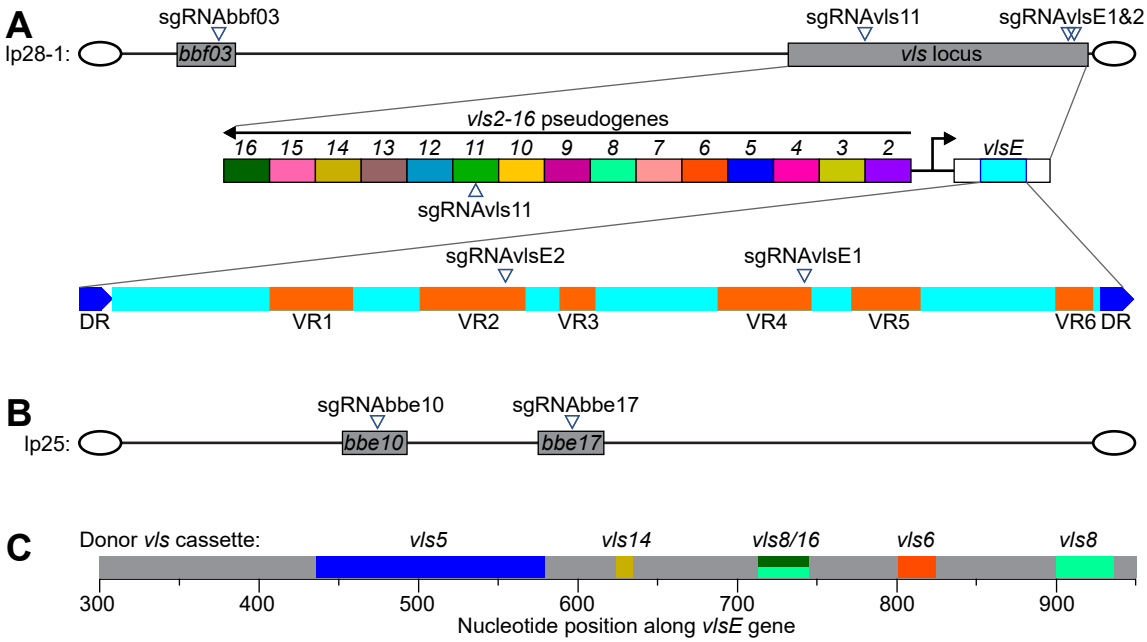

Figure 3

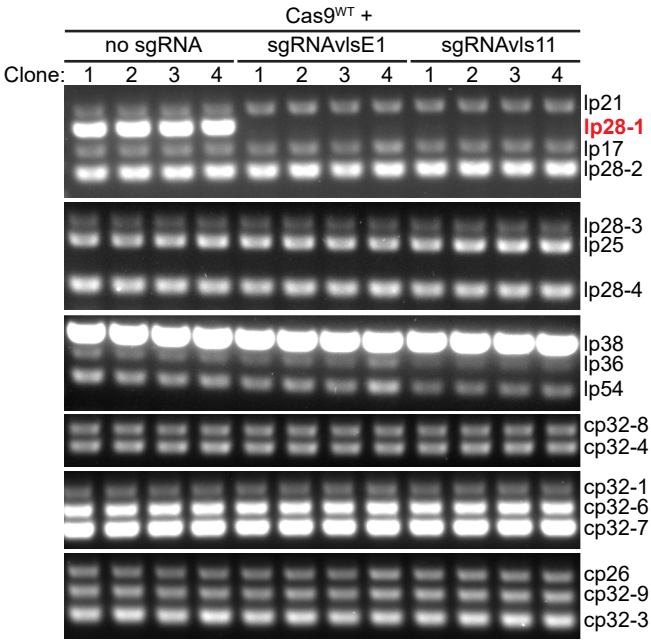

Figure 4

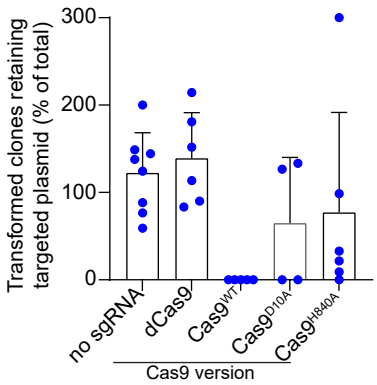

Figure S1